Oxidative Stress, Mitochondrial Perturbations and Fetal Programming of Renal Disease induced by Maternal Smoking

Stefanie Stangenberg[1], Long T Nguyen[2], Hui Chen[2], Ibrahim Al-Odat[2], Murray C Killingsworth[3], Martin E Gosnell[4], Ayad G Anwer[4], Ewa M Goldys[4], Carol A Pollock[1], Sonia Saad[1*]

[1]Kolling Institute of Medical Research, Royal North Shore Hospital, Sydney Medical School, University of Sydney, St Leonards, NSW, Australia

[2]School of Medical and Molecular Biosciences, Faculty of Science, Centre for Health Technology, University of Technology, Sydney, Australia

[3]Department of Anatomical Pathology, Sydney South West Pathology Service, Liverpool Australia

[4]MQ BioFocus Research Centre, Macquarie University, Sydney, NSW Australia

Corresponding author*

Dr Sonia Saad

Department of Medicine

Kolling Institute of Medical Research

University of Sydney, NSW, Australia

Tel +61 2 9926 4782

Fax +61 2 9926 5715

Email: sonia.saad@sydney.edu.au

Running title: Fetal programming of kidney disease

ABSTRACT

An adverse in-utero environment is increasingly recognized to predispose to chronic disease in adulthood. Maternal smoking remains the most common modifiable adverse in-utero exposure leading to low birth weight, which is strongly associated with chronic kidney disease (CKD) in later life. In order to investigate underlying mechanisms for such susceptibility, female Balb/c mice were sham or cigarette smoke-exposed (SE) for 6 weeks before mating, throughout gestation and lactation. Offspring kidneys were examined for oxidative stress, expression of mitochondrial proteins, mitochondrial structure as well as renal functional parameters on postnatal day 1, day 20 (weaning) and week 13 (adult age). From birth throughout adulthood, SE offspring had increased renal levels of mitochondrial-derived reactive oxygen species (ROS), which left a footprint on DNA with increased 8-Hydroxydeoxyguanosin (8-OHdG) in kidney tubular cells. Mitochondrial structural abnormalities were seen in SE kidneys at day 1 and week 13 along with a reduction in oxidative phosphorylation (OXPHOS) proteins and activity of mitochondrial antioxidant Manganese superoxide dismutase (MnSOD). Smoke exposure also resulted in increased mitochondrial DNA copy number (day 1-week 13) and lysosome density (day 1 and week 13). The appearance of mitochondrial defects preceded the onset of albuminuria at week 13. Thus, mitochondrial damage caused by maternal smoking may play an important role in development of CKD at adult life.

Keywords: renal fibrosis, maternal effects, oxidative stress, smoking, mitochondrial function

1. INTRODUCTION

The theory of fetal programming which links chronic adulthood diseases to adverse conditions in early life is an intriguing concept, which is increasingly recognized. Low birth weight is a surrogate marker for such unfavorable conditions in-utero and is strongly associated with development of chronic kidney disease (CKD) in later life (White et al., 2009). The prevalence of end-stage kidney disease continues to increase (Coresh et al., 2007) and is not always explained by traditional risk factors. In fact, it often remains unclear why the rate of CKD progression shows substantial variation from patient to patient even among individuals with similar comorbidities. Although a reduced nephron endowment has been implicated (Brenner et al., 1988, Hoy et al., 2005) the underlying molecular mechanisms for fetal programming of adult onset kidney disease are largely unknown.

Maternal smoking remains the most common modifiable adverse fetal exposure leading to low birth weight and other adverse fetal outcomes (Andres and Day, 2000, Jaddoe et al., 2008). Despite a recent decrease in smoking rates in developed countries, according to the 2010 Pregnancy Risk Assessment and Monitoring System (PRAMS) data from 27 states in the United States approximately 10.7% of women reported smoking during the last three months of pregnancy (Tong et al., 2013). Epidemiological studies have shown that maternal smoking alters the in-utero growth pattern of kidneys and leads to a reduced kidney volume in fetal and postnatal life (Lampl et al., 2005, Taal et al., 2011). Using a mouse model of maternal smoke exposure, we have shown that offspring of SE mothers had delayed glomerular development at an early postnatal period, with adaptively enlarged glomerulus size and albuminuria in adulthood (Al-Odat, 2014).

Cigarette smoke is a major source of reactive oxygen species (ROS). High concentrations of ROS cause lipid peroxidation, damage to cell membranes, proteins, and DNA. Evidence is mounting that maternal smoking causes an increase in oxidative stress in fetal cord blood and placenta (Aydogan et al., 2013, Sbrana et al., 2011). Mitochondria are the main intracellular source but also a primary target of ROS, which are generated as by-products of ATP synthesis through the oxidative phosphorylation system (OXPHOS). Mitochondria serve a crucial role in development by providing energy for the rapid fetal growth (May-Panloup et al., 2007). Disruption of mitochondrial homeostasis may lead to long-lasting detrimental effects and failure of organ function over time. The role of mitochondrial dysfunction and ROS production is clearly established in a number of chronic adult onset diseases including Parkinson's disease (Jenner, 2001), Alzheimer's disease (Aliev et al., 2003), atherosclerosis (Harrison et al., 2011), diabetes (Green et al., 2004, Nishikawa et al., 2000) as well as aging (Huang and Manton, 2004, Sastre et al., 2000). Evidence for mitochondrial dysfunction in chronic kidney disease is emerging from high throughput genome-based microarray technology (Granata et al., 2009) and a number of experimental studies (Su et al.,

2013, Yuan et al., 2012a, Zhang et al., 2007, Zhu et al., 2011). It remains to be shown whether the mitochondrial perturbations are present already at birth as a consequence of an adverse in-utero environment.

The present study was designed to test the hypothesis that maternal smoking causes increased ROS production and mitochondrial perturbations in renal tissue in the offspring at birth and that this effect is sustained into adulthood.

2. MATERIALS AND METHODS

2.1. In vivo experiment

2.1.1. Animal smoking model. The study was approved by the Animal Care and Ethics Committee of the University of Technology, Sydney (ACEC #2011-313A). Female Balb/c mice (Animal Resources Centre, Perth, Australia) were housed at 20±2°C, and maintained on a 12:12h light/dark cycle (lights on 06:00h), with free access to water and standard laboratory chow (11kJ/g, Gordon's Specialty Stockfeeds, NSW, Australia). Twice daily (5 days/week) they underwent smoke exposure (SE) in a Perspex chamber with smoke generated from 2 cigarettes (nicotine≤1.2mg, CO≤15mg) for 6 weeks before mating, throughout gestation and lactation. The control sham-exposed mice were put in an identical chamber for the same period. During lactation the offspring remained in the home cage without SE. Pups were weighed every 5 days and weaned at postnatal day 20. A terminal urine collection was undertaken via direct bladder puncture at the end points: day 1, day 20 (weaning) and week 13 (mature age). Blood was collected via cardiac puncture after mice were anesthetized. Plasma was separated immediately and stored at -20°C for creatinine measurements. Then animals were sacrificed by cervical dislocation. Kidneys were harvested, snap frozen and stored at -80° for further processing. Only male offspring were used for this study.

2.2 Mitochondrial marker

2.2.1. Mitochondrial protein extraction. The protein extraction method was derived from the Calbiochem superoxide dismutase assay kit II (Merck Millipore, Darmstadt, Germany) that was subsequently used to assess superoxide dismutase (SOD) activity. Mitochondrial protein fractions were obtained by differential centrifugation. Prior to protein extraction, tissue was rinsed with phosphate buffered saline (PBS), pH7.4, containing 0.16mg/ml heparin to remove any red blood cells and clots. Tissue was homogenized with a Quiagen TissueRuptur (Quiagen, Limburg, Netherlands) in 1.5 ml of cold 20mM HEPES buffer, pH 7.2, containing 1mM EGTA, 210mM mannitol, 70mM sucrose and centrifuged at 1500g for 5 min at 4°C. The supernatant was centrifuged for 15 min at 10000g at 4°C. The pellet containing the mitochondrial fraction was suspended in 20mM HEPES buffer, pH 7.2 with 1mM EGTA, 210mM mannitol and 70mM

sucrose. The purity of the mitochondrial fraction was tested by determining the expression of the mitochondrial specific protein VDAC in cytosolic and mitochondrial extracts. Protein quantification (BioRad, CA, USA) was carried out to determine the protein concentration.

2.2.2. Western blot of mitochondrial proteins. 10 μg of protein were mixed with 4X Loading buffer, 10X reducing agent (Life Technologies, Vic, Australia) and water to make 20 μl solutions; and heated at 70°C for 10 min. Samples were then analysed by SDS gel electrophoresis (Life Technologies, Vic, Australia) and electroblotted to Hybond Nitrocellulose membranes (Amersham Pharmacia Biotech, Bucks, UK). Membranes were blocked in Tris-buffered saline containing 0.2% Tween-20 (TBST) in 5% skim milk for 30 min and then incubated overnight at 4°C with the following primary antibodies: MitoProfil Total OXPHOS Rodent WB antibody cocktail 1:250 (Abcam Ltd, Cambridge, UK), TOM20 1:500 (Santa Cruz, CA, USA), MnSOD 1:1000 (Millipore, Billerica, MA, USA) in TBST containing 5% skim milk. Membranes were washed with TBST and incubated with horseradish peroxidase conjugated secondary antibody. Proteins were visualized using Luminata Western HRP Substrate (Millipore, MA, USA) in a LAS 4000 image reader (Fujifilm, Tokyo, Japan). All membranes were re-probed with β-actin 1:1000 (Santa Cruz, CA, US) and results were expressed as percentage of protein expression relative to β-actin. Analysis was performed using Image J software (Java based software program, National Institutes of Health).

2.2.3. Determination of Mitochondrial MnSOD activity. The activity of MnSOD was determined in the mitochondrial protein fraction by a standard kit from Calbiochem (Merck Millipore, Darmstadt, Germany) following the manufacturer's instructions. The MnSOD activity was expressed as the amount of enzyme causing a 50% inhibition of formazan dye, employing hypoxanthine and xanthine oxidase to generate superoxide radicals.

2.2.4. Electron microscopy of mitochondria. Kidney tissue was fixed in 2.5% glutaraldehyde in 0.1M sodium cacodylate buffer pH7.4 and subsequently sliced into 100 nm thick ultrathin sections, then mounted on 300 mesh copper grids for imaging of mitochondria with an FEI Morgagni 268D transmission electron microscope (FEI, Eindhoven, The Netherlands).

2.2.5. Mitochondrial copy number. Genomic DNA was extracted from renal tissue using the DNeasy blood and tissue kit (Quiagen). The content of mtDNA was calculated using real-time quantitative PCR by measuring the threshold cycle ratio (ΔCt) of the mitochondrial-encoded gene cytochrome c oxidase subunit 1 (COX1), (forward primers 5′-ACTATACTACTACTAA-CAGACCG-3′, reverse primers 5′-GGTTCTTTTTTTCCGGAGTA-3′) versus the nuclear-encoded

gene cyclophilin A (forward primers 5′-ACACGCCATAATGGCACTGG-3′, reverse primers 5′-CAGTCTTGGCAGTGCAGAT-3′).

2.3 Oxidative stress markers

2.3.1. Confocal Microscopy. Frozen kidney sections were stained and imaged using Leica SP2 confocal laser scanning microscope (Leica, Wetzlar, Germany). Data was generated from three independent experiments, each in triplicates. Fifty images were taken from each slide and averaged before the analysis. All imaging parameters including laser intensities, Photomultiplier tubes voltage, pinhole were kept constant during imaging. For total ROS detection, CellROX Deep Red (Molecular Probes, Australia) was used at 5 µM final concentration, images were collected at 633 nm excitation wavelength and detected in the 640-680 nm emission range. MitoTracker Green (Molecular Probes, Australia) was used to visualize the mitochondria at 200nM final concentration. Images were collected at 458 nm excitation wavelength and detected in the 480-505nm emission range. Lysosomes were visualized using LysoTracker Red DND-99 (Molecular Probes, Australia) with 100 nM final concentration. Images were collected at 514 nm excitation wavelength and detected in the 525-550nm emission range. To calculate the correlation between CellROX and Mitotracker, dual staining using CellRox and Mitotracker was performed and images were taken sequentially using separate confocal channels over a time not greater than 30 seconds. The image pixel intensity value correlation was then calculated using Pearson's correlation for all pixels excluding any pairs containing zero values.

2.3.2. Immunohistochemistry. Formalin-fixed paraffin-embedded sections were deparaffinized and boiled for 20 min in 10mM citrate buffer (pH 6.0). Sections were washed in TBST and exposed to 0.3% H_2O_2 for 5 min to quench endogenous peroxidases. Immunohistochemistry was performed using the following antibody: rabbit anti-8OHdG polyclonal antibody (1:100, BIOSS, Woburn, MA, USA). Concentration-matched rabbit IgG was used as an isotype-negative control. The sections were blocked with Dako proteinblock (Dako, Carpinteria, CA, USA) for 10 min and incubated with primary antibody overnight. The slides were then incubated with horseradish peroxidase anti-rabbit Envision–system followed by a 3.3’-diaminobenzidine (DAB) substrate-chromogen solution (Dako) and counterstained with Harris hematoxylin. The slides were examined using a Leica photomicroscope linked to a DFC 480 digital camera (Leica, Wetzlar, Germany).
The quantitation was performed by capturing 6-10 non-overlapping fields of renal cortex from stained sections. Areas of brown staining reflecting 8-OHdG were highlighted using a selective color tool and the proportional area of the field with their respective color range was quantified using Image J.

2.4. Statistical analysis

All results are expressed as mean ± standard error (SE) and statistical significance was defined as $P < 0.05$. Experiments were performed at least in three independent experiments or as detailed in the text with n reflecting the number of separate experiments. Statistical comparisons between groups were made by unpaired student t-tests or non-parametric Mann-Whitney U test. Analyses were performed using the software package, GraphPad Prism version 6 (GraphPad Software Inc, La Jolla, California, USA). For the confocal study, the data distribution was assesses using a non-parametric test of different source distributions (Kolmogorov-Smirnov) which is sensitive to difference in the shape and position of the empirical distribution functions of the compared samples and is particularly useful where there is doubt regarding the nature of the source population (Lehmann and Romano, 2005). Multiple images were taken for over 100 cells in each tissue in 3 replicates of 3 independent samples/group. Pearson's correlation method was used to determine the correlation factor and p values for the correlation study.

3. RESULTS

3.1. Physiological and renal parameters.

The physiological characteristics of mice offspring are summarized in table 1. In keeping with the known effect of maternal nicotine exposure during gestation we observed a reduced birth weight (day 1) in offspring of smoke-exposed mothers with normalization of weight at weaning (day 20) and adulthood (week 13). Kidney weight was similarly reduced at day 1 in the SE offspring but had normalized by day 20. Serum creatinine remained normal in both groups at adulthood, however offspring of smoke-exposed mothers developed an increased urinary albumin/creatinine ratio at week 13.

3.2. Increased mitochondrial oxidative stress in offspring kidneys from smoke- exposed mothers.

Products from cigarette smoke are known inducers of oxidative stress in various tissues and are able to cross the placenta. In order to investigate whether maternal smoking causes oxidative stress in the offspring, frozen renal sections were co-stained with CellRox Red and Mitotracker Green. There was a significant increase of total ROS in SE offspring at day 20 and week 13 ($P<0.001$; Figure 1A and 1C). The correlation coefficient of the mean fluorescent intensities was significantly higher in the kidney of the SE offspring at day 1 and week 13 ($P < 0.01$, Figure 1B and 1D) suggesting that at these time points ROS was localized within or within close proximity to the mitochondria.

3.3. Increased DNA oxidation in offspring kidneys from smoke-exposed mothers.

As high levels of ROS can cause damage to DNA, we next performed immunohistochemistry for 8-hydroxydeoxyguanosin (8-OHdG), which is formed when DNA is oxidatively modified by ROS. A significant increase of 8-OHdG in paraffin-embedded kidney sections from smoke-exposed offspring was observed at all time points. Both proximal and distal tubules stained positive for 8-OHdG with sparing of the glomeruli. The most intense staining was noted in distal tubules with predominantly cytoplasmic staining (Figure 2).

3.4. Reduced mitochondrial MnSOD in offspring kidneys from smoke-exposed mothers at postnatal day 1 and week 13.

SOD is a crucial component of the cellular antioxidant defense. While other isoforms of SOD are located in the cytosol, MnSOD is mostly located in the mitochondria. In order to determine MnSOD activity, mitochondrial protein fractions were obtained by differential centrifugation. MnSOD activity was significantly reduced at day 1 and week 13 ($P < 0.05$) but not at day 20 (Figure 3).

3.5. Reduced renal OXPHOS protein subunits in offspring kidneys from smoke-exposed mothers

To investigate mitochondrial protein expression, we looked at TOM20, a mitochondrial outer membrane receptor for translocation of cytosolically synthesized mitochondrial pre-proteins, and subunits of the OXPHOS complexes I – V, key components of the mitochondrial respiratory chain for ATP synthesis. TOM20 was significantly reduced in offspring from SE mothers at day 1 and week 13 ($P<0.01$ and $P<0.001$ respectively, Fig 4). There was no change in TOM20 protein levels at day 20. In addition, there was a significant reduction in subunits of complex I, II, III and V both at postnatal day 1 and week 13 in the SE offspring compared to control (Figure 5A and 5C). At day 1 the most marked differences were observed in complex V ($p<0.01$). However, at weaning age (day 20) there was no significant difference in any of the mitochondrial enzyme subunits, which may suggest a regenerative effect during lactation and consequent to the high levels of antioxidants in breast milk. At mature age (week 13) there was again a significant protein reduction in all of the examined OXPHOS subunits. The most pronounced reduction at week 13 was observed in complex II, IV and V ($P<0.01$, Figure 5C).

3.6. Increased mitochondrial DNA copy number in offspring from smoke-exposed mothers.

It has been suggested, that abnormal amounts of mitochondrial DNA, either depletion or elevation, are associated with mitochondrial dysfunction. We thus investigated mitochondrial copy number in SE offspring. Our data showed that offspring DNA from SE mothers have increased levels of mitochondrial-encoded Cox1/ nuclear-encoded cyclophillin at postnatal day 1, day 20 and week 13

(P < 0.05 vs control, Figure 6). This suggests that maternal smoke exposure increases mitochondrial density/mass due to either increased mitochondrial size or number.

3.7. Alteration of mitochondrial ultrastructure in smoke-exposed offspring.

Renal mitochondria structure was examined using electron microscopy. Offspring kidneys from control mice had normal mitochondrial morphology as demonstrated by long filamentous mitochondria. In contrast, offspring from SE mothers exhibit mitochondrial enlargement and swelling at day 1 and week 13. Additionally, an increased number of small punctate mitochondria at day 1 and week 13 was also evident suggesting increased mitochondrial fragmentation. However, this effect was not evident in the SE offspring at day 20 (Figure 7).

3.8. Increased mitochondrial density in offspring kidneys from smoke-exposed mothers.

Using Mitotracker, a mitochondrial selective fluorescent probe, we confirmed that the cellular mitochondrial density is significantly increased in offspring kidney from SE mothers at day 1 and week 13 compared to control (P<0.05 and P<0.001vs control, Figure 8). However, there was a reduction (P<0.05 vs control) in the mitochondrial density at day 20.

3.9. Increased lysosome density in offspring from smoke-exposed mothers

Defective mitochondria are engulfed in autophagosomes that fuse with lysosomes. In order to investigate whether maternal smoke exposure induces mitophagy, lysosomal density was determined. Lysosome density significantly increased in offspring from SE mothers at week 13 (P<0.001 versus control; Figure 9). As was evident in the divergent results for the offspring at weaning for the above parameters, the mean cellular lysosome levels were significantly decreased in offspring from SE mothers at day 20 (P<0.001 versus control; Figure 9).

4. DISCUSSION

The present study demonstrates increased renal oxidative stress, reduced mitochondrial antioxidant activity as well as mitochondrial structural changes and reduced OXPHOS proteins in offspring of SE mothers at birth and adulthood. This is associated with an increased urinary albumin to creatinine ratio in adulthood. The presence of albuminuria suggests renal pathology independent of glomerular filtration rate, and independently portends an accelerated decline in kidney function in all forms of kidney disease (Iseki, 2013).

Our study suggests that fetal programming of CKD is regulated, at least in part, by maternal tobacco smoke-mediated production of oxidative stress and mitochondrial perturbations. The

presence of mitochondrial dysfunction in the placenta of smoking mothers has previously been demonstrated (Bouhours-Nouet et al., 2005). To our knowledge, this is the first study showing enhanced oxidative stress and mitochondrial changes in offspring kidney tissue following maternal cigarette exposure. A previous animal study in Wistar rats similarly demonstrated increased ROS formation and altered mitochondrial structure in adult offspring pancreatic tissue in response to maternal subcutaneous injections of nicotine during gestation and lactation (Bruin et al., 2008). Bruin et al. found that mitochondrial structural defects were accompanied by a modest decline in OXPHOS complex IV activity at adult age. In accordance with our results, Bruin et al. observed mitochondrial structural abnormalities as early as three weeks after birth (weaning age), which progressively worsened even though nicotine exposure was discontinued at weaning. Importantly these changes preceded decreased pancreatic beta cell function and glucose intolerance in adult life highlighting again the role of fetal programming in the development of chronic adulthood diseases. In an atherosclerosis mouse model using Apolipoprotein E null mice, Fetterman et al. demonstrated that in-utero smoke exposure significantly accelerated adult atherosclerosis. Consistent with our findings, the smoke-exposed offspring showed increased oxidative stress and a reduction in MnSOD levels at an adult age, which was associated with increased mitochondrial DNA copy number and the presence of mitochondrial DNA deletions in aorta tissue (Fetterman et al., 2013).

The mitochondrial genome is more susceptible to ROS induced DNA damage than the nuclear genome and exhibits higher rates of DNA mutation due to the lack of histone protection, reduced DNA repair capacity and close proximity to the ROS producing electron transport chain. However, it is suggested that even in the absence of detectable mitochondrial DNA mutations, alterations in mitochondrial DNA content, either depletion or elevation, may be an indicator of mitochondrial dysfunction (Bai et al., 2004). In this study we detected an increase in mitochondrial DNA content in SE offspring. The mechanism by which mitochondrial DNA increases in response to oxidative stress is not well understood. It is hypothesized that this is a compensatory mechanism for the decline in mitochondrial function by inducing the proliferation of mitochondria and/ or mitochondrial DNA amplification (Bai et al., 2004, Lee et al., 2000). An increase in mitochondrial DNA levels have been shown in vitro in response to oxidative stress (Al-Kafaji and Golbahar, 2013, Lee et al., 2000), in age related mitochondrial alterations (Barrientos et al., 1997, Lee et al., 1998) and in smokers (Ballinger et al., 1996, Lee et al., 1998, Masayesva et al., 2006). Masayesva et al. detected not only an age-independent elevation of mitochondrial DNA levels in current smokers but also in former smokers with mean cessation intervals of two decades (Masayesva et al., 2006). The persistence of these changes is consistent with our in-utero smoke exposure model where elevated mitochondrial DNA content was detectable long after birth.

When DNA is oxidatively modified by ROS, the amount of 8-OHdG increases. Our data confirmed that smoke exposure induces oxidative modification of DNA in the offspring from birth and this was persistent till adulthood. The fact that 8-OHdG was increased in the cytoplasm suggests increased oxidative damage to the mitochondrial DNA (Nomoto et al., 2008). Although 8-OHdG was increasingly expressed in the proximal tubule, its level of expression was more intense in distal tubules. A possible explanation is the fact that ROS detoxifying enzymes are more abundant in proximal tubular cells than distal tubules, which may indicate a diminished ability to detoxify reactive metabolites in this part of the nephron and a higher intrinsic susceptibility of distal tubular cells to oxidative injury (Lash and Tokarz, 1990).

Although we detected DNA oxidation and changes in mitochondrial DNA copy number in smoke-exposed offspring persistently from day 1 till week 13, mitochondrial structural changes and OXPHOS as well as TOM20 protein depletion were seen at birth and adulthood without any significant change at day 20. MnSOD protein content and activity mirrored the OXPHOS protein content changes with a significant MnSOD reduction demonstrated at day 1 and week 13 and equally no significant change at weaning age. We propose that the deleterious effects on mitochondria observed at birth and in adulthood may be mitigated at weaning due to the antioxidants in the breast milk (Ermis et al., 2005, Zagierski et al., 2012). Further studies to investigate this hypothesis are needed.

MnSOD is the primary mitochondrial ROS scavenging enzyme that transforms toxic superoxide free radicals to hydrogen peroxide, which is subsequently converted to water by catalases and other peroxidases. MnSOD has also recently been demonstrated to be part of a protein complex necessary for mitochondrial DNA repair (Bakthavatchalu et al., 2012), thus playing a pivotal role in multiple aspects of mitochondrial protection. Cigarette smoke has previously been shown to reduce MnSOD levels in circulating blood cells (Mandraffino et al., 2010), while in-utero smoke exposure caused a reduction of MnSOD levels in aortic tissue in the offspring (Fetterman et al., 2013). This study is the first to demonstrate reduced MnSOD levels in offspring kidneys in response to maternal smoking. Of note is the occurrence of reduced MnSOD levels in offspring long after smoke exposure at adulthood both in our model and in the study of Fetterman et al.(Fetterman et al., 2013) highlighting the long-term toxic effects of cigarette smoke as the basis for fetal programming.

Using electron microscopy we have demonstrated in proximal tubular cells, that offspring from SE mothers exhibit mitochondrial enlargement and had an increased number of small punctate

mitochondria at day 1 and week 13 suggestive of increased mitochondrial fragmentation. The presence of structural mitochondrial abnormalities is in accordance with other studies of direct smoke exposure (Hara et al., 2013) and in-utero nicotine exposure (Bruin et al., 2008). Damaged mitochondria are removed by mitophagy, a selective autophagy process, during which autophagosomes enclose whole mitochondria, or selectively target damaged areas and fuse with lysosomes for degradation. Cellular lysosome density was increased in SE offspring at day 1 and week 13. This suggests that smoke exposure induces accumulation of damaged mitochondria and may impair mitophagy but this requires further investigation.

Mitochondria serve a crucial role in development by providing energy for the rapid fetal growth and play key roles in cell signaling (Duchen, 2004, May-Panloup et al., 2007). Environmental exposures that result in mitochondrial perturbations have long-lasting effects and may lead to failure of organ function over time. The kidney is a highly metabolic organ and rich in mitochondria. There is increasing evidence implicating mitochondrial dysfunction in the pathogenesis of chronic kidney disease (CKD) and acute kidney injury (AKI). Genomic analysis of blood samples from CKD patients revealed differential expression of genes encoding OXPHOS and reduced complex IV activity (Granata et al., 2009). Mitochondrial dysfunction has been implicated as an early event in experimentally induced podocyte dysfunction (Yuan et al., 2012b) as well as epithelial to mesenchymal transition (EMT), which is a major mechanism leading to renal tubulointerstitial fibrosis (Yuan et al., 2012a, Zhang et al., 2007). In AKI it is increasingly recognized that cell death is disproportionately low despite often severely impaired renal function (Takasu et al., 2013, Tran et al., 2011). Subtle vacuolization in proximal tubular cells are often the only documented structural lesions and are considered to represent swollen mitochondria (Takasu et al., 2013, Tran et al., 2011). Several studies have shown a reduction of OXPHOS protein and activity in experimental models of AKI (Funk and Schnellmann, 2012, Rasbach and Schnellmann, 2007). Our data suggests that maternal smoking induces mitochondrial perturbations and possibly dysfunction, although this was not directly investigated. Additional functional experiments are needed to validate this finding.
We demonstrated the occurrence of albuminuria at adult age in offspring of smoke exposed mothers. Albuminuria as an early marker for kidney damage is also an independent predictor for an accelerated progression of chronic kidney disease to more advanced stages. The effect of smoking on development of albuminuria is well described (Halimi et al., 2000, Hogan et al., 2007, Pinto-Sietsma et al., 2000) however the effect of prenatal smoke exposure on offspring kidneys is less studied. An experimental study on offspring rats exposed to cigarette-smoke condensate in-utero revealed lower glomerular volume and glomerular cells compared to control (Zarzecki et al., 2012). In contrast to our study this study did not show a difference between smoke exposed offspring and

control with respect to birth weight, kidney weight, albuminuria or creatinine clearance. The lack of reduced birth weight may signal lower levels of smoke exposure. The smoke exposure was different to our model with oral mucosa application of cigarette-smoke condensate dissolved in acetone containing nicotine. While there was high nicotine exposure as evidenced by the increased cotinine levels, the amount of other toxins in the condensate may have been less than in our model. A more recent study also found that smoke exposure in utero has pro-fibrotic influences on offspring kidneys (Chen et al., 2015). Although we did not detect any renal histological changes at any time point (data not shown) nor an increase in serum creatinine, we propose that our findings of mitochondrial alterations at birth and adulthood may put offspring at increased risk for renal pathology especially in the setting of additional insults, such as sepsis or toxins. A history of maternal smoke exposure in-utero may thus predispose to more severe forms of AKI or irreversible damage that leads to progression of CKD. The results of this study highlight the importance of optimization of maternal and fetal health as well as smoking prevention. It remains to be shown whether the negative impact on mitochondrial integrity can be reversed or potentially avoided by smoking cessation prior to pregnancy.

ACKNOWLEDGEMENTS

We thank Dr. Jie Zhang (Kolling Institute of Medical Research) for her technical support. E.M.G., M.E.G. and A.G.A acknowledge partial support from the Australian Research Council Centre of Excellence Scheme (CE140100003).

STATEMENT OF COMPETING FINANCIAL INTERESTS

None of the authors has a financial disclosure.

REFERENCES

Al-Kafaji G, Golbahar J. High glucose-induced oxidative stress increases the copy number of mitochondrial DNA in human mesangial cells. BioMed research international. 2013;2013:754946.
Al-Odat I, Hui, C, Chan, Y-L, Wong, MG, Gill, A, Pollock, CA, Saad, S. The impact of maternal cigarette smoke exposure in a rodent model on renal development in the offspring. PloS one. 2014.
Aliev G, Seyidova D, Lamb BT, Obrenovich ME, Siedlak SL, Vinters HV, et al. Mitochondria and vascular lesions as a central target for the development of Alzheimer's disease and Alzheimer disease-like pathology in transgenic mice. Neurological research. 2003;25:665-74.
Andres RL, Day MC. Perinatal complications associated with maternal tobacco use. Seminars in neonatology : SN. 2000;5:231-41.
Aydogan U, Durmaz E, Ercan CM, Eken A, Ulutas OK, Kavuk S, et al. Effects of smoking during pregnancy on DNA damage and ROS level consequences in maternal and newborns' blood. Arhiv za higijenu rada i toksikologiju. 2013;64:35-46.
Bai RK, Perng CL, Hsu CH, Wong LJ. Quantitative PCR analysis of mitochondrial DNA content in patients with mitochondrial disease. Annals of the New York Academy of Sciences. 2004;1011:304-9.
Bakthavatchalu V, Dey S, Xu Y, Noel T, Jungsuwadee P, Holley AK, et al. Manganese superoxide dismutase is a mitochondrial fidelity protein that protects Polgamma against UV-induced inactivation. Oncogene. 2012;31:2129-39.
Ballinger SW, Bouder TG, Davis GS, Judice SA, Nicklas JA, Albertini RJ. Mitochondrial genome damage associated with cigarette smoking. Cancer research. 1996;56:5692-7.
Barrientos A, Casademont J, Cardellach F, Ardite E, Estivill X, Urbano-Marquez A, et al. Qualitative and quantitative changes in skeletal muscle mtDNA and expression of mitochondrial-encoded genes in the human aging process. Biochemical and molecular medicine. 1997;62:165-71.
Bouhours-Nouet N, May-Panloup P, Coutant R, de Casson FB, Descamps P, Douay O, et al. Maternal smoking is associated with mitochondrial DNA depletion and respiratory chain complex III deficiency in placenta. American journal of physiology Endocrinology and metabolism. 2005;288:E171-7.
Brenner BM, Garcia DL, Anderson S. Glomeruli and blood pressure. Less of one, more the other? American journal of hypertension. 1988;1:335-47.
Bruin JE, Petre MA, Raha S, Morrison KM, Gerstein HC, Holloway AC. Fetal and neonatal nicotine exposure in Wistar rats causes progressive pancreatic mitochondrial damage and beta cell dysfunction. PloS one. 2008;3:e3371.
Chen CM, Chou HC, Huang LT. Maternal nicotine exposure during gestation and lactation induces kidney injury and fibrosis in rat offspring. Pediatric research. 2015;77:56-63.
Coresh J, Selvin E, Stevens LA, Manzi J, Kusek JW, Eggers P, et al. Prevalence of chronic kidney disease in the United States. Jama. 2007;298:2038-47.
Duchen MR. Mitochondria in health and disease: perspectives on a new mitochondrial biology. Molecular aspects of medicine. 2004;25:365-451.
Ermis B, Yildirim A, Ors R, Tastekin A, Ozkan B, Akcay F. Influence of smoking on serum and milk malondialdehyde, superoxide dismutase, glutathione peroxidase, and antioxidant potential levels in mothers at the postpartum seventh day. Biological trace element research. 2005;105:27-36.
Fetterman JL, Pompilius M, Westbrook DG, Uyeminami D, Brown J, Pinkerton KE, et al. Developmental exposure to second-hand smoke increases adult atherogenesis and alters mitochondrial DNA copy number and deletions in apoE(-/-) mice. PloS one. 2013;8:e66835.
Funk JA, Schnellmann RG. Persistent disruption of mitochondrial homeostasis after acute kidney injury. American journal of physiology Renal physiology. 2012;302:F853-64.
Granata S, Zaza G, Simone S, Villani G, Latorre D, Pontrelli P, et al. Mitochondrial dysregulation and oxidative stress in patients with chronic kidney disease. BMC genomics. 2009;10:388.
Green K, Brand MD, Murphy MP. Prevention of mitochondrial oxidative damage as a therapeutic strategy in diabetes. Diabetes. 2004;53 Suppl 1:S110-8.

Halimi JM, Giraudeau B, Vol S, Caces E, Nivet H, Lebranchu Y, et al. Effects of current smoking and smoking discontinuation on renal function and proteinuria in the general population. Kidney international. 2000;58:1285-92.
Hara H, Araya J, Ito S, Kobayashi K, Takasaka N, Yoshii Y, et al. Mitochondrial fragmentation in cigarette smoke-induced bronchial epithelial cell senescence. American journal of physiology Lung cellular and molecular physiology. 2013;305:L737-46.
Harrison CM, Pompilius M, Pinkerton KE, Ballinger SW. Mitochondrial oxidative stress significantly influences atherogenic risk and cytokine-induced oxidant production. Environmental health perspectives. 2011;119:676-81.
Hogan SL, Vupputuri S, Guo X, Cai J, Colindres RE, Heiss G, et al. Association of cigarette smoking with albuminuria in the United States: the third National Health and Nutrition Examination Survey. Renal failure. 2007;29:133-42.
Hoy WE, Hughson MD, Bertram JF, Douglas-Denton R, Amann K. Nephron number, hypertension, renal disease, and renal failure. J Am Soc Nephrol. 2005;16:2557-64.
Huang H, Manton KG. The role of oxidative damage in mitochondria during aging: a review. Frontiers in bioscience : a journal and virtual library. 2004;9:1100-17.
Iseki K. Chronic kidney disease: Proteinuria as a predictor of rapid eGFR decline. Nature reviews Nephrology. 2013;9:570-1.
Jaddoe VW, Troe EJ, Hofman A, Mackenbach JP, Moll HA, Steegers EA, et al. Active and passive maternal smoking during pregnancy and the risks of low birthweight and preterm birth: the Generation R Study. Paediatric and perinatal epidemiology. 2008;22:162-71.
Jenner P. Parkinson's disease, pesticides and mitochondrial dysfunction. Trends in neurosciences. 2001;24:245-7.
Lampl M, Kuzawa CW, Jeanty P. Growth patterns of the heart and kidney suggest inter-organ collaboration in facultative fetal growth. American journal of human biology : the official journal of the Human Biology Council. 2005;17:178-94.
Lash LH, Tokarz JJ. Oxidative stress in isolated rat renal proximal and distal tubular cells. The American journal of physiology. 1990;259:F338-47.
Lee HC, Lu CY, Fahn HJ, Wei YH. Aging- and smoking-associated alteration in the relative content of mitochondrial DNA in human lung. FEBS letters. 1998;441:292-6.
Lee HC, Yin PH, Lu CY, Chi CW, Wei YH. Increase of mitochondria and mitochondrial DNA in response to oxidative stress in human cells. The Biochemical journal. 2000;348 Pt 2:425-32.
Lehmann EL, Romano JP. Testing statistical hypotheses. Third edition. Springer Texts in Statistics Springer New York. 2005:584-90.
Mandraffino G, Sardo MA, Riggio S, D'Ascola A, Loddo S, Alibrandi A, et al. Smoke exposure and circulating progenitor cells: evidence for modulation of antioxidant enzymes and cell count. Clinical biochemistry. 2010;43:1436-42.
Masayesva BG, Mambo E, Taylor RJ, Goloubeva OG, Zhou S, Cohen Y, et al. Mitochondrial DNA content increase in response to cigarette smoking. Cancer epidemiology, biomarkers & prevention : a publication of the American Association for Cancer Research, cosponsored by the American Society of Preventive Oncology. 2006;15:19-24.
May-Panloup P, Chretien MF, Malthiery Y, Reynier P. Mitochondrial DNA in the oocyte and the developing embryo. Current topics in developmental biology. 2007;77:51-83.
Nishikawa T, Edelstein D, Du XL, Yamagishi S, Matsumura T, Kaneda Y, et al. Normalizing mitochondrial superoxide production blocks three pathways of hyperglycaemic damage. Nature. 2000;404:787-90.
Nomoto K, Tsuneyama K, Takahashi H, Murai Y, Takano Y. Cytoplasmic fine granular expression of 8-hydroxydeoxyguanosine reflects early mitochondrial oxidative DNA damage in nonalcoholic fatty liver disease. Applied immunohistochemistry & molecular morphology : AIMM / official publication of the Society for Applied Immunohistochemistry. 2008;16:71-5.

Pinto-Sietsma SJ, Mulder J, Janssen WM, Hillege HL, de Zeeuw D, de Jong PE. Smoking is related to albuminuria and abnormal renal function in nondiabetic persons. Annals of internal medicine. 2000;133:585-91.
Rasbach KA, Schnellmann RG. PGC-1alpha over-expression promotes recovery from mitochondrial dysfunction and cell injury. Biochemical and biophysical research communications. 2007;355:734-9.
Sastre J, Pallardo FV, Vina J. Mitochondrial oxidative stress plays a key role in aging and apoptosis. IUBMB life. 2000;49:427-35.
Sbrana E, Suter MA, Abramovici AR, Hawkins HK, Moss JE, Patterson L, et al. Maternal tobacco use is associated with increased markers of oxidative stress in the placenta. American journal of obstetrics and gynecology. 2011;205:246 e1-7.
Su M, Dhoopun AR, Yuan Y, Huang S, Zhu C, Ding G, et al. Mitochondrial dysfunction is an early event in aldosterone-induced podocyte injury. American journal of physiology Renal physiology. 2013;305:F520-31.
Taal H, Geelhoed J, Steegers E, Hofman A, Moll H, Lequin M, et al. Maternal smoking during pregnancy and kidney volume in the offspring: the Generation R Study. Pediatric Nephrology. 2011:1-9.
Takasu O, Gaut JP, Watanabe E, To K, Fagley RE, Sato B, et al. Mechanisms of cardiac and renal dysfunction in patients dying of sepsis. American journal of respiratory and critical care medicine. 2013;187:509-17.
Tong VT, Dietz PM, Morrow B, D'Angelo DV, Farr SL, Rockhill KM, et al. Trends in smoking before, during, and after pregnancy--Pregnancy Risk Assessment Monitoring System, United States, 40 sites, 2000-2010. Morbidity and mortality weekly report Surveillance summaries (Washington, DC : 2002). 2013;62:1-19.
Tran M, Tam D, Bardia A, Bhasin M, Rowe GC, Kher A, et al. PGC-1alpha promotes recovery after acute kidney injury during systemic inflammation in mice. The Journal of clinical investigation. 2011;121:4003-14.
White SL, Perkovic V, Cass A, Chang CL, Poulter NR, Spector T, et al. Is low birth weight an antecedent of CKD in later life? A systematic review of observational studies. American journal of kidney diseases : the official journal of the National Kidney Foundation. 2009;54:248-61.
Yuan Y, Chen Y, Zhang P, Huang S, Zhu C, Ding G, et al. Mitochondrial dysfunction accounts for aldosterone-induced epithelial-to-mesenchymal transition of renal proximal tubular epithelial cells. Free radical biology & medicine. 2012a;53:30-43.
Yuan Y, Huang S, Wang W, Wang Y, Zhang P, Zhu C, et al. Activation of peroxisome proliferator-activated receptor-gamma coactivator 1alpha ameliorates mitochondrial dysfunction and protects podocytes from aldosterone-induced injury. Kidney international. 2012b;82:771-89.
Zagierski M, Szlagatys-Sidorkiewicz A, Jankowska A, Krzykowski G, Korzon M, Kaminska B. Maternal smoking decreases antioxidative status of human breast milk. Journal of perinatology : official journal of the California Perinatal Association. 2012;32:593-7.
Zarzecki M, Adamczak M, Wystrychowski A, Gross ML, Ritz E, Wiecek A. Exposure of pregnant rats to cigarette-smoke condensate causes glomerular abnormalities in offspring. Kidney & blood pressure research. 2012;36:162-71.
Zhang A, Jia Z, Guo X, Yang T. Aldosterone induces epithelial-mesenchymal transition via ROS of mitochondrial origin. American journal of physiology Renal physiology. 2007;293:F723-31.
Zhu C, Huang S, Yuan Y, Ding G, Chen R, Liu B, et al. Mitochondrial dysfunction mediates aldosterone-induced podocyte damage: a therapeutic target of PPARgamma. The American journal of pathology. 2011;178:2020-31.

FIGURE LEGENDS

Figure 1. Detection of oxidative stress. (A) CellROX stain for total ROS in frozen renal sections of offspring mice of smoke-exposed mothers (SE) and control at postnatal day 1, day 20 and week 13. (B) Dual staining for CellROX and Mitotracker showing that most ROS in offspring kidneys from SE mothers, was localized within or within close proximity to the mitochondria at day 1 and week 13. (C) Quantitative representation of Mean Fluorescent Intensity (MFI) for ROS. (D) Pixel intensity scatter plots showing correlation between Mitotracker (green) and CellRox (red) in offspring kidney from control and SE mothers at day 1, day 20 and week 13. Data are expressed as mean± SEM, n= 3, **P < 0.01, ***P < 0.001 using non parametric test of different source distributions (Kolmogrov-Smirnov). Correlation factor and P values for the correlation study (Figure 1D) was determined using Pearson Correlation. Colours (green, red and yellow) reflect Mitotracker, CellRox and colocalised pixels. Scale bars represent 50μm.

Figure 2. Immunostaining of 8-OHdG in paraffin sections of renal tissue. (A) Representative images of renal cortex showing 8-OHdG expression at day 1, day 20 and week 13. Black arrows and white arrows showed increased expression of 8-OHdG in representative distal tubules and proximal tubules respectively. Original magnification: x 200 (B) Quantitation of 8-OHdG. Data is expressed as mean % of stained area ±SEM, n=5-6 *P < 0.05 vs control mice using unpaired t tests. Scale bars represent 50μm

Figure 3. Mitochondrial MnSOD activity in offspring kidney at postnatal day 1, day 20 and week 13. Results are expressed as mean ± SEM, n=6-8; *P<0.05 vs. control using unpaired t tests.

Figure 4. Renal TOM 20 levels and representative blot in offspring kidney at day 1, day 20 and week 13. Results are normalized to β-actin which was detectable in mitochondrial fractions and did not change with experimental conditions. Results are expressed as mean ± SEM, n=6-8. **P < 0.01, ***P < 0.001 vs. control using unpaired t tests.

Figure 5. Renal OXPHOS complex I – V levels in mitochondrial protein fractions of offspring from control and smoke-exposed mothers at postnatal day 1 (A), day 20 (B) and week 13 (C). (D) Representative blots for OXPHOS complex I-V at day 1, day 20 and week 13. Results are normalized to β-actin which was detectable in mitochondrial fractions and did not change with experimental conditions. Results are expressed as mean ± SEM, n=6-8. *P < 0.05, **P < 0.01 vs. control using unpaired t tests.

Figure 6. Mitochondrial DNA copy number shown by the ratio of mitochondrial-encoded COX1 to nuclear-encoded cyclophilin A in offspring renal DNA from control and smoke-exposed mothers at postnatal day 1, day 20 and week 13. Results are expressed as fold increase ± SEM, n=4; *P<0.05 vs. control using non parametric Mann-Whitney U test.

Figure 7. Electron microscopic detection of mitochondria in offspring renal proximal tubular cells from control and smoke-exposed mothers at day 1, day 20 and week 13.
Normal looking (long filamentous) mitochondria are shown in offspring kidney from control mothers at day 1, day 20 and week 13 and in kidneys from SE mothers at day 20. White arrows show enlarged (circular shaped) mitochondria and black arrows show increased number of small punctate mitochondria at day 1 and week 13 in offspring kidney from SE mothers.
Insets in the far left corner: high magnification view of mitochondria. Scale bar =10,000 nm.

Figure 8. Mitotracker staining showing mitochondrial mean fluorescence intensity (MFI) in offspring kidney at postnatal day 1, day 20 and week 13. Increased mitochondrial density is shown in offspring kidney from SE mothers at day 1 and week 13. Results are expressed as mean ± SEM, n=3; *P < 0.05, *** P < 0.001 vs. control using non parametric test of different source distributions (Kolmogrov-Smirnov). Scale bars represent 50μm.

Figure 9. Mean fluorescence intensity (MFI) for Lysotracker stain in offspring kidney from control and smoke-exposed mothers at postnatal day 1, day 20, and week 13.

Increased lysosomal density is shown in offspring kidney from SE mothers at day 1 and week 13. Data is expressed as mean ± SEM, n=3, *P < 0.05, ***P < 0.001 vs. control using non parametric test of different source distributions (Kolmogrov-Smirnov). Scale bars represent 50μm.

Table 1. Characteristics of offspring mice. Data are expressed as mean ± SEM of 5-10 male mice per group. *P < 0.05 vs. control using unpaired t tests.

TABLES

Table 1

	Control	SE
Day 1		
Body weight (g)	1.55 ± 0.05	1.35 ± 0.06*
Kidney weight (g)	0.0081 ± 0.0004	0.0069 ± 0.0004*
Kidney/body weight (%)	0.52 ± 0.02	0.51 ± 0.04
Day 20		
Body weight (g)	9.97 ± 0.16	9.71 ± 0.14
Kidney weight (g)	0.067 ± 0.001	0.062 ± 0.003
Kidney/body weight (%)	0.67 ± 0.01	0.64 ± 0.03
Albumin/creatinine ratio (μg/mg)	8.69 ± 2.00	6.12 ± 1.45
Serum creatinine (μmol/l)	10.4 ± 0.7	12.1 ± 1.2
Week 13		
Body weight (g)	25.5 ± 0.3	25.1 ± 0.6
Kidney weight (g)	0.20 ± 0.01	0.19 ± 0.01
Kidney/body weight (%)	0.77 ± 0.01	0.76 ± 0.02
Albumin/creatinine ratio (μg/mg)	7.00 ± 2.3	38.0 ± 6.3*
Serum creatinine (μmol/l)	15.2 ± 1.3	14.2 ± 0.5

FIGURES

Figure 1.

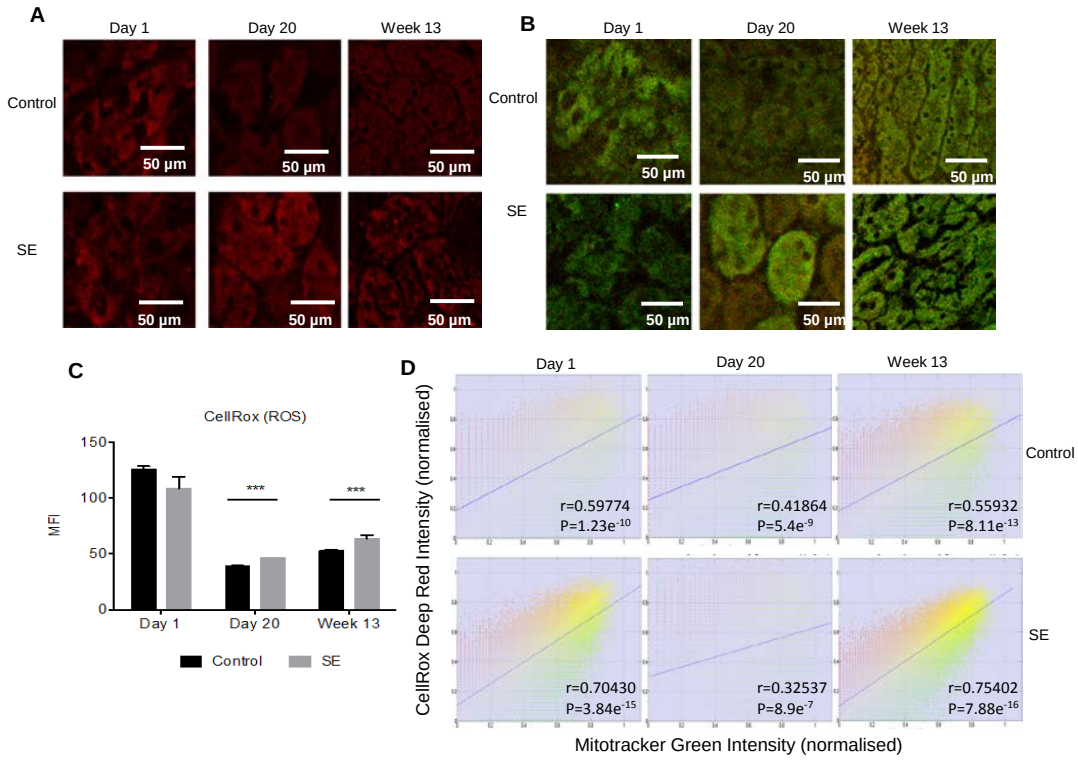

Figure 2.

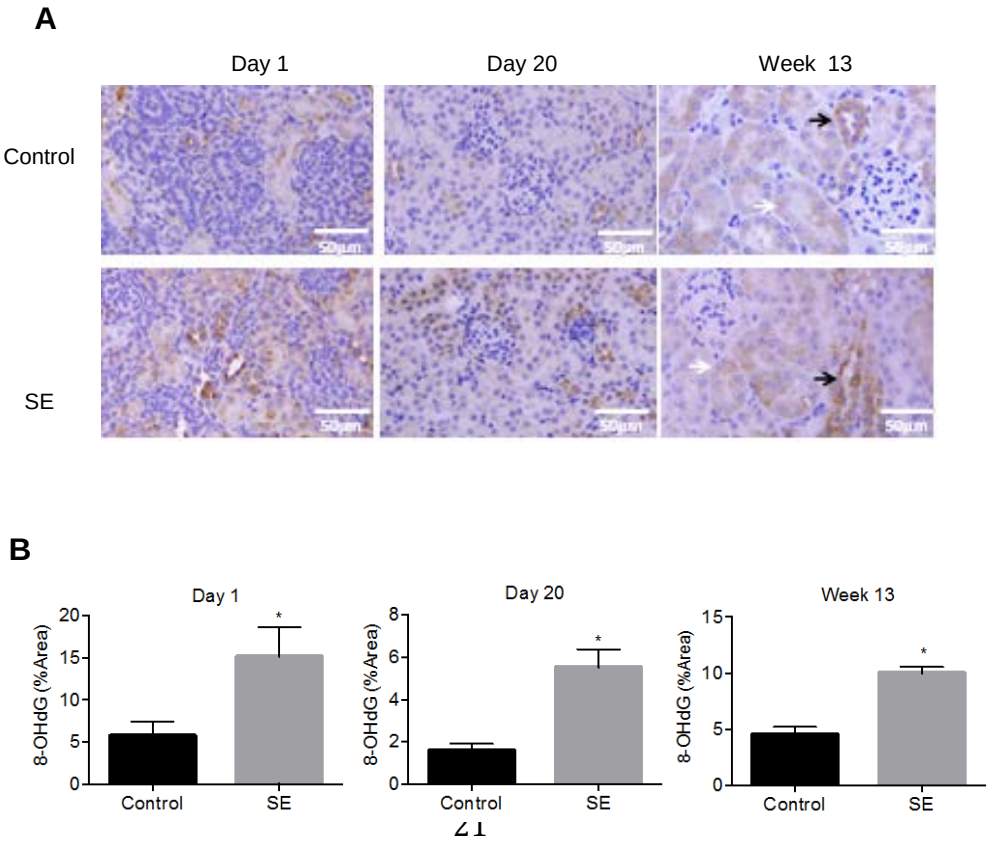

Figure 3.

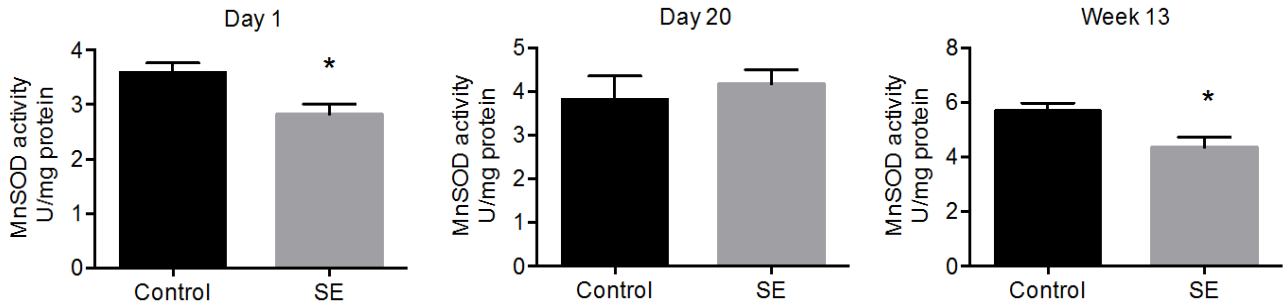

Figure 4.

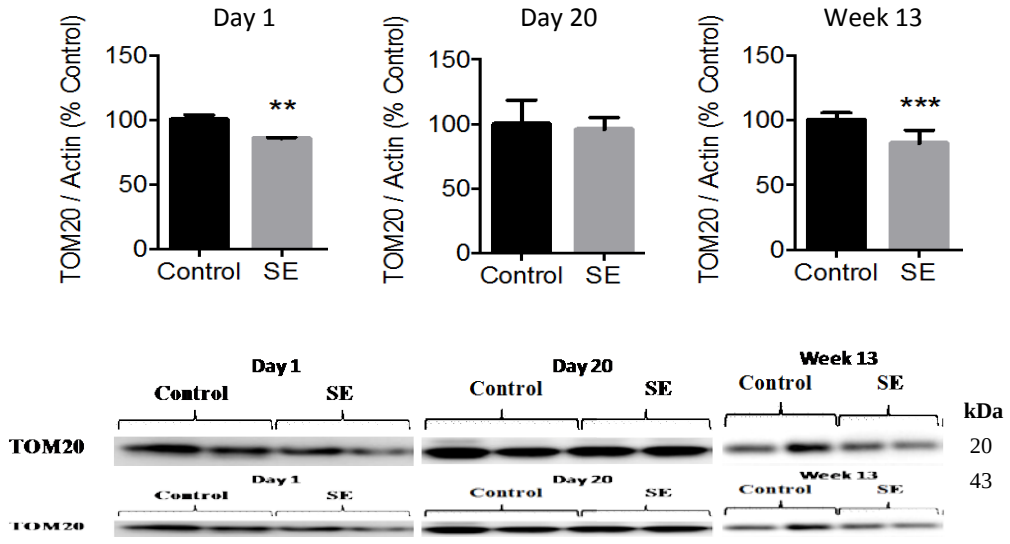

Figure 5.

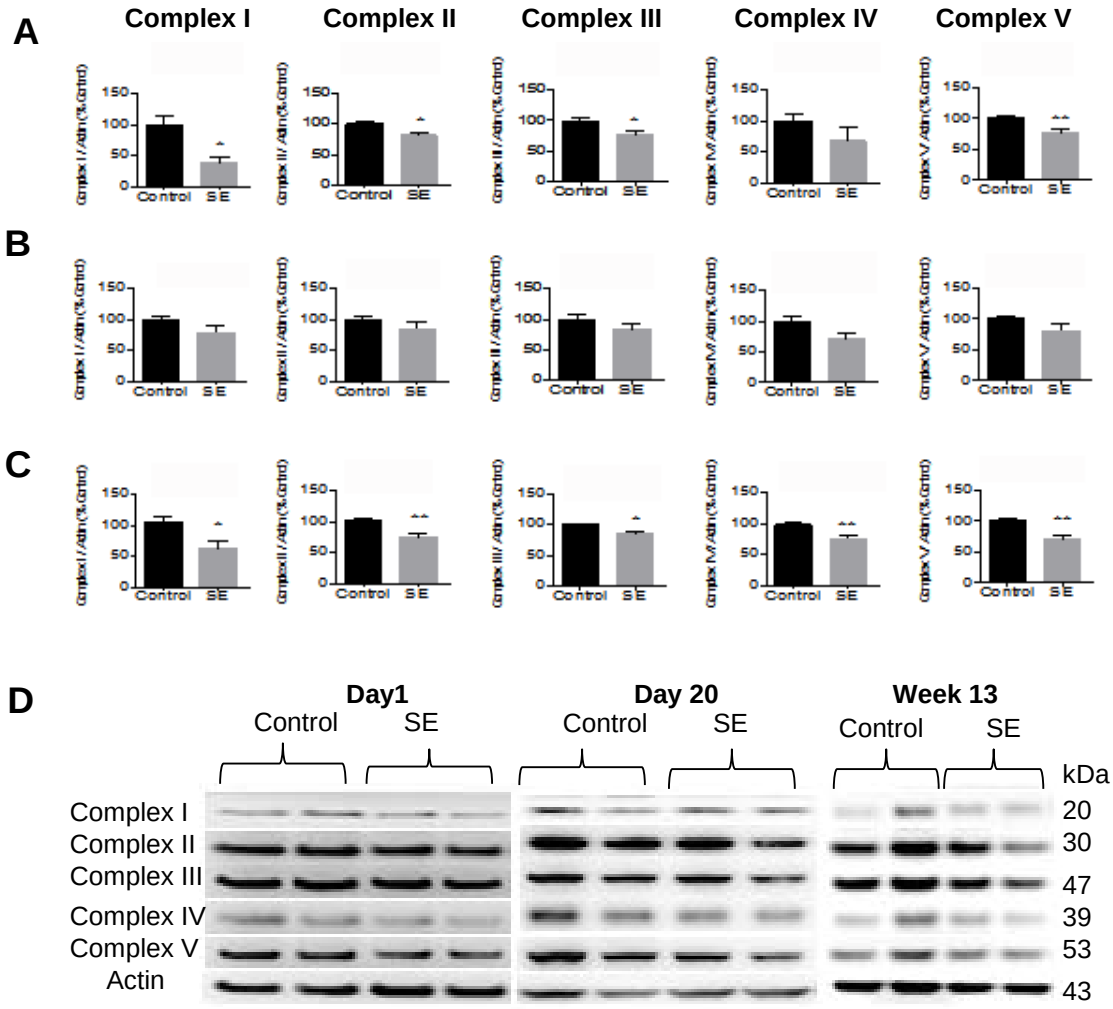
A
Complex I
Complex II
Complex III
Complex IV
Complex V
B
C
D
Day1
Day 20
Week 13
Control
SE
kDa
Complex I
Complex II
Complex III
Complex IV
Complex V
Actin
20
30
47
39
53
43

Figure 6.

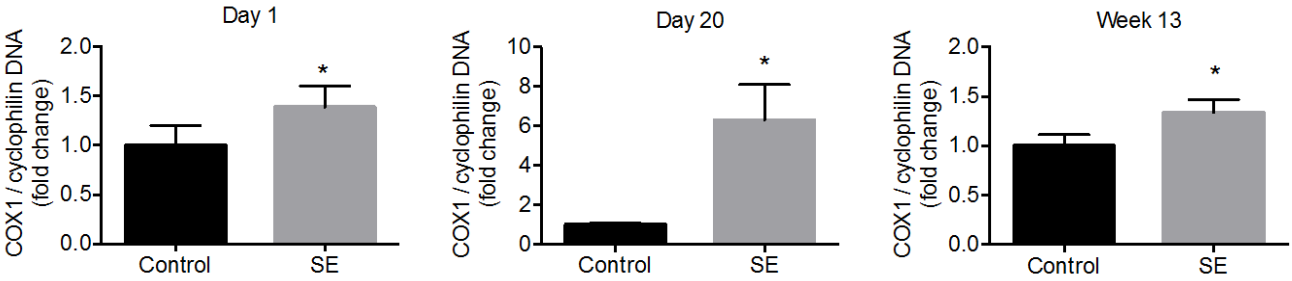

Figure 7.

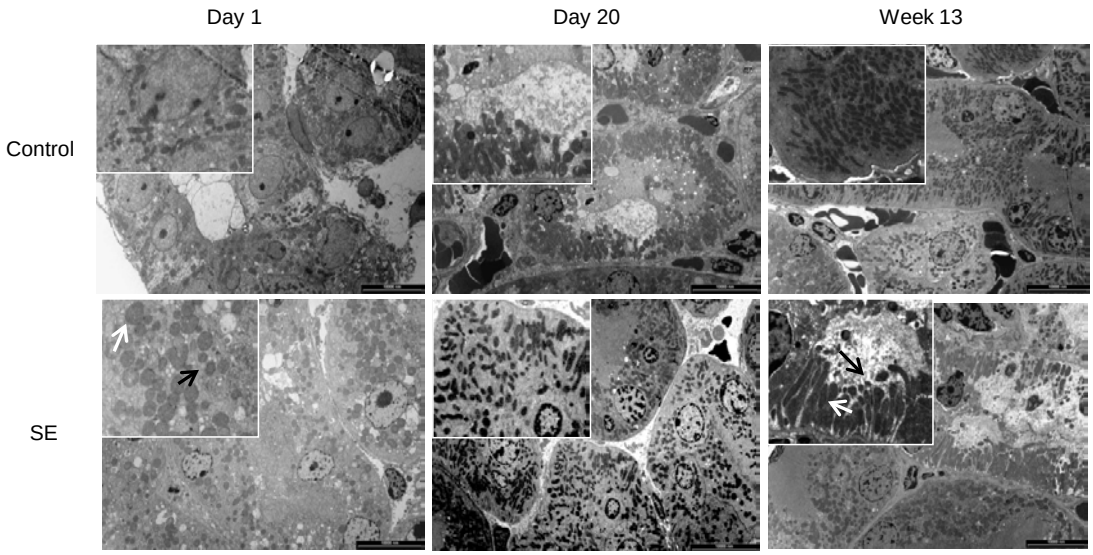

Figure 8.

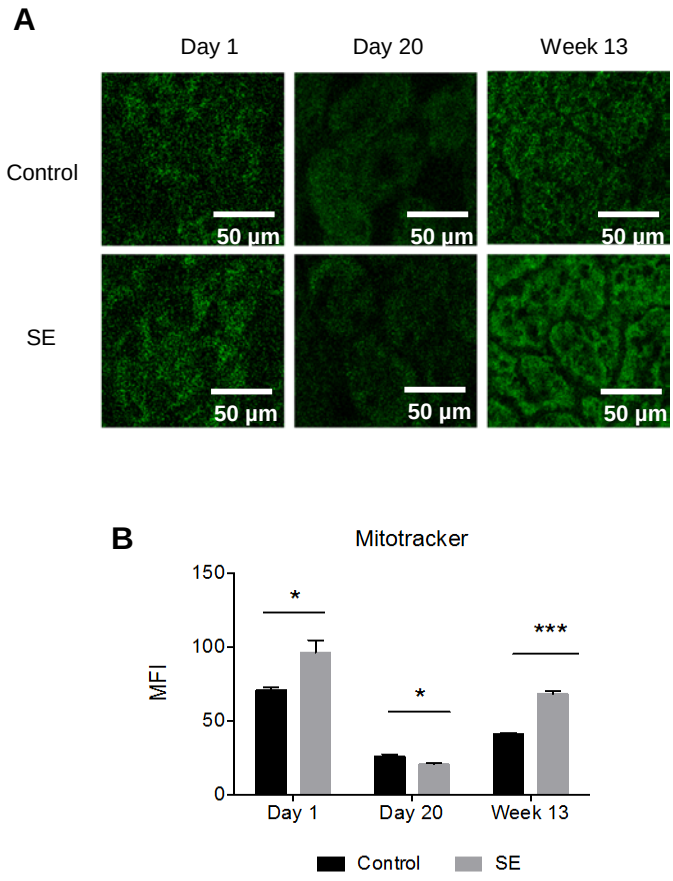
A
Day 1
Day 20
Week 13
Control
SE
50 µm
B
Mitotracker
MFI
150
100
50
0
*
*
***
Day 1
Day 20
Week 13
Control
SE

Figure 9.

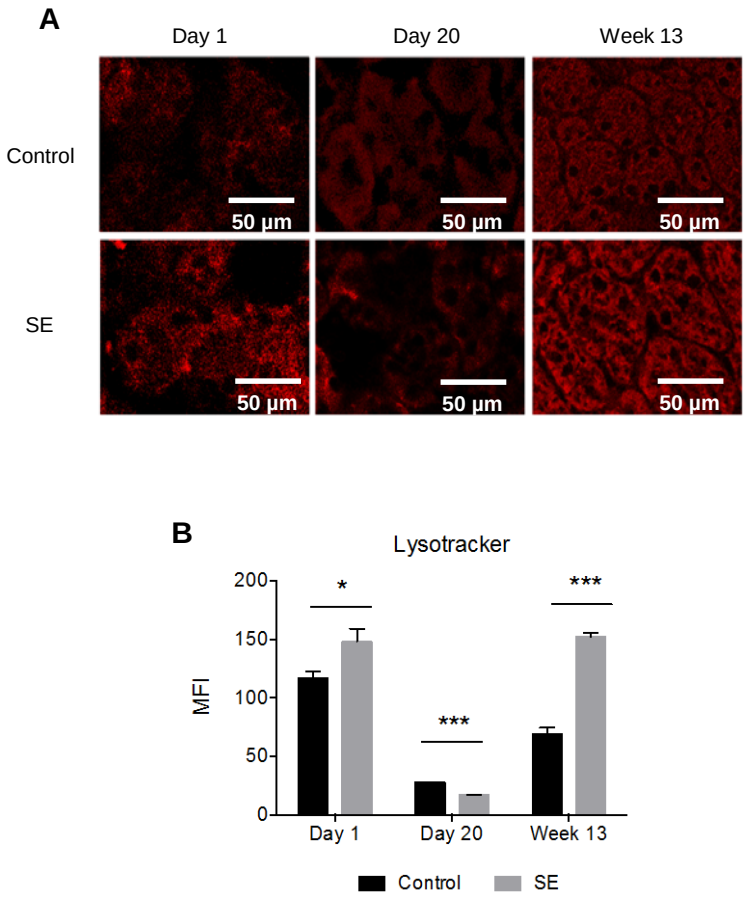
A
Day 1
Day 20
Week 13
Control
SE
50 µm
B
Lysotracker
MFI
200
150
100
50
0
*
***
***
Day 1
Day 20
Week 13
Control
SE